J Mater Sci (2007) 42:5766–5772
DOI 10.1007/s10853-006-1153-x

Effect of oxygen partial pressure on the electrical and optical properties of highly (200) oriented p-type $Ni_{1-x}O$ films by DC sputtering

Suman Nandy · Biswajit Saha · Manoj K. Mitra · K. K. Chattopadhyay

Received: 28 June 2006 / Accepted: 16 October 2006 / Published online: 20 April 2007

Abstract Thin films of NiO (bunsenite) with (200) preferential orientation were synthesized on glass substrates by direct current sputtering technique in Ar+O_2 atmosphere. Nanostructural properties of the NiO films were investigated by X-ray diffraction and also by atomic force microscopic (AFM) studies. Electrical and optical properties of the deposited films were investigated as a function of different partial pressure of oxygen in the sputtering gas mixture during deposition. The films showed p-type electrical conduction and the conductivity depends on the partial pressure of oxygen. The electrical conductivity (σ_{RT}) was found to be .0615 S cm^{-1} for films deposited with 100% O_2 and its value sharply decreased with the decrease the partial pressure of O_2; for example σ_{RT} for 50% O_2 was 6.139×10^{-5} S cm^{-1}. The mechanism of the origin of p-type electrical conductivity in the NiO film is discussed from the viewpoint of nickel or oxygen vacancies, which generate holes and electrons respectively. X-ray photoelectron spectroscopic studies supported the above argument. Corresponding optical properties showed that the transparency decreases with increasing oxygen partial pressure and the bandgap also decreases.

S. Nandy · B. Saha · K. K. Chattopadhyay
Thin Film & Nanoscience Laboratory, Department of Physics, Jadavpur University, Kolkata 700 032, India

M. K. Mitra · K. K. Chattopadhyay (✉)
Nanoscience and Technology Center, Jadavpur University, Kolkata 700 032, India
e-mail: kalyan_chattopadhyay@yahoo.com

Introduction

Nickel oxide (NiO), with excellent chemical stability, having a wide band gap in the range 3.6–4.0 eV [1], as well as interesting optical, electrical and magnetic properties, has immense potential in a number of applications. NiO thin films have been widely investigated as a promising material for the possible applications in spin-valve giant magneto resistance (GMR) sensor [2–5], gas sensors [6], chemical sensors [7], electrochromic display devices [8], p-type transparent conducting electrodes [9] etc. NiO has a rock salt crystalline structure (i.e NaCl-type structure) and has a lattice constant of 0.417 nm. Numerous attempts including sputtering [10, 11], electron beam evaporation [12, 13], and sol-gel technique [14] have been used for the synthesis of NiO thin films. NiO thin films usually exhibit p-type conduction due to holes generated by Ni vacancies in the lattice. Recently, various theoretical methods for the calculation of the electronic states in NiO, using Low Spin Density Approximation (LSDA), LSDA + U, or GW approximation can be found in the literature [15, 16]. However, the behavior of NiO as a p-type semiconductor is not yet fully understood. Also, the electronic structure of NiO makes it an interesting candidate for material research.

The electrical conductivity of undoped NiO has a strong dependence on the formation of microstructural defects, such as nickel vacancies and interstitial oxygen in NiO crystallites [17]. With proper thermal treatment, it becomes slightly non-stoichiometric, acquiring an excess of oxygen, which is compensated by the oxidation of some Ni^{2+} to Ni^{3+}. In the ground state the extra charge of Ni^{3+} is trapped close to the Ni vacancy [18] and can move only by an activated hopping process similar to that exhibited by ionic diffusion. Therefore this kind of compound is generally denoted as a hopping semiconductor [19]. By controlling

the resistivity and thickness of NiO thin films, it is expected to enhance the utility in current applications as well as creating new ones. Literature survey indicated that the synthesis of NiO film by dc sputtering of NiO target is scanty and more work is necessary to decipher its conduction mechanism. In this paper we have investigated the electrical and optical properties of direct current sputter deposited highly oriented NiO thin films as a function of oxygen partial pressure.

Experimental procedure

Target preparation for sputtering

NiO target for the sputtering was fabricated by compacting nickel oxide powder (99.99%, Sigma Aldrich) taking in a grooved aluminium holder of 5 cm diameter and applying a suitable hydrostatic pressure (~100 kg/cm^2). The fabricated NiO target was placed in the DC sputtering chamber for the deposition of nanocrystalline thin films on glass and Si substrates for different partial pressure of oxygen in the sputtering gas mixture.

Film synthesis and characterization

DC Sputtering [20] is a well known technique for the deposition of thin films. For the synthesis of NiO thin films we used DC sputtering for different partial pressure of oxygen in the oxygen + argon gas mixture, keeping the other sputtering parameters unaltered (substrate temperature, substrate to target distance, HT power, deposition time etc.). Both the argon and oxygen gas flows were controlled by mass flow controllers. Although bulk NiO is not really a good conductor and hence DC sputtering is not usually attempted for the synthesis of NiO thin film. The reason of origin of moderate conductivity of NiO is the presence of excess oxygen as NiO is a defect semiconductor. During sputtering in oxygen atmosphere (either 100% or less) the resistivity of the NiO target decreased due to increase of oxygen concentration in the lattice. Hence although the sputtering rate was not as good as in the case of a conducting target an average moderate sputtering rate of ~5 nm/min was achieved by DC sputtering.

The chamber was initially evacuated by a standard rotary and diffusion pumping arrangement to a base pressure of 10^{-6} mbar and the sputtering pressure was 0.2 mbar. Table 1 gives the details of sputtering parameters used during deposition. For all the films, the deposition time was 150 min and the substrate temperature was kept at 350 °C. X-ray diffraction pattern was recorded by an X-ray diffractometer (Bruker D8 Advance) in the 2θ range 20–70° using CuK_α radiation (λ = 0.15406 nm) operated at 40 kV and 40 mA. A UV-Vis-NIR spectrophotometer (Shimadzu-UV-3101-PC) was used to determine the optical properties. It is a double beam spectrophotometer with integrating sphere attachment for reflectance measurement within the wavelength range of 190–2600 nm. The bond vibrational energy of Ni–O was determined by a Fourier-transformed infrared spectrometer (FTIR, Shimadzu 8400S). The surface morphology of NiO thin film was studied by an atomic force microscope (NT-MDT, Solver Pro) with the scanning region 25 μm^2. The sheet resistance and temperature dependence of the electrical conductivity of the films were studied by a linear four-probe method using a Kiethley electrometer (Model 6514) from 300 K to 550 K. The thickness of the films varied in range 700–800 nm with the increase of oxygen partial pressure (as measured by cross sectional SEM measurement, not shown here) for the same deposition time of 150 min. Considering the correct thickness of each film, the electrical conductivity was calculated. X-ray photoelectron spectra were recorded by an XPS system (Specs, Germany) with a hemispherical analyzer (HSA-3500).

Results and discussion

Crystalline structure

XRD analysis

Figure 1 shows the XRD patterns of the nickel oxide (NiO) film deposited on glass substrates for different oxygen partial pressure. It is seen from the XRD pattern that the crystalline structure of cubic NiO (bunsenite) film is highly (200) oriented with $a_0 = b_0 = c_0 = 4.178$ [21]. The relatively sharp (200) diffraction peaks imply that the films have a good quality of crystallinity and preferential orientation. Fig. 1 indicates that as the partial pressure of oxygen increases, the (200) peak intensity of NiO thin films also increases. It is also noticeable from the XRD pattern that the NiO thin films showed crystallinity even when the oxygen partial pressure is 0; i.e. the films were deposited only in Ar atmosphere. This is in contradiction with the results reported by Lee et al. [22] who indicated that the crystallinity was achieved only when the percentage of oxygen was greater than 3%. From the XRD pattern using Sherrer equation we get the particle size of NiO thin films are around 10–11.7 nm.

AFM studies and FTIR analysis

An atomic force microscope was used for scanning a 5 μm × 5 μm area of the NiO films for examining the

Table 1 Details of deposition parameters

Electrode distance	1.5 cm
Sputtering pressure	0.2 mbar
Substrate	Glass and Si
Deposition time	150 min
Substrate temperature	350 °C
Sputtering voltage	2 kV
Current density	1.5 mA/cm^2
Volume percentages of O_2	100%, 80%, 70%, 50%, 20%, 0%

surface morphology. From the AFM images (not shown here) the particle size of NiO was also obtained and it was observed that the particle size has a sharp distribution having a mean value ~15 nm.

The Ni–O orbitals are formed by the overlapping between the $3d^8$ and $4s^2$ orbitals of Ni atom and the $2p^4$ orbitals of the O atom. From the orbital diagram of ground state of NiO, as shown schematically in Fig. 2, it can be seen that the δ^4 orbital is nonbonding, $d\sigma^2$ and π^2 orbitals are weakly antibonding and the remaining orbitals ($\sigma^2\pi^4$) are bonding. There are also nonbonding $4s\sigma^2$ orbitals formed from the valance 4s orbitals of Ni [23–28, 29]. The ground electronic state is known to be a $^3\Sigma^-$ state having an electronic configuration that can be approximately described as .... $(8\sigma)^2(3\pi)^4(1\delta)^4(9\sigma)^2(4\pi)^2$ [28] with substantial ionic character. FTIR spectra (not shown here) of the films deposited on Si substrates clearly showed absorptions bands corresponding to vibrational mode of Ni–O bonds. The observed peak was at around 848 cm^{-1} which is assigned due to the bond vibration of Ni–O at ground state [29] and another peak at 666 cm^{-1} for anion state [29].

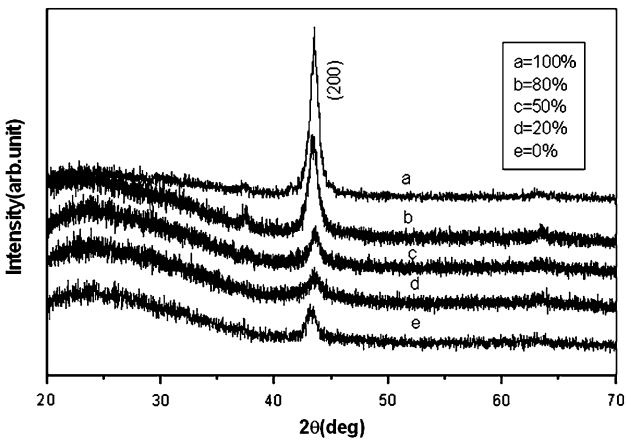

Fig. 1 XRD pattern of NiO thin film on glass substrate for different partial pressure of oxygen

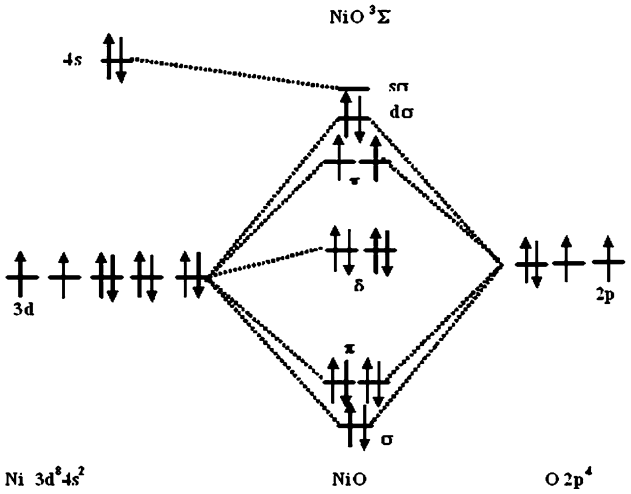

Fig. 2 Schematic diagram showing molecular orbital diagram of the $^3\Sigma^-$ ground state of NiO showing the mixing of atomic O and Ni orbitals

Electrical conductivity measurements

Figure 3 represents the temperature variation (from 300 K to 575 K) of the electrical conductivity (σ) of the films for different percentage of oxygen (100%, 80%, 70% and 50%) present in the sputtering gas at a constant substrate temperature of 350 °C. An increase of the room-temperature conductivity (σ_{RT}) was observed with the increase in partial pressure of O_2. It was seen that at the presence of 100% O_2 the σ_{RT} is 0.0615 S cm^{-1} and it sharply decreases with the decrease of partial pressure of O_2; σ_{RT} for 50% O_2 is nearly about 6.139×10^{-5} S cm^{-1}. For films deposited with 0% O_2 the electrical conductivity of the film was so low that we could not measure in our conductivity setup. From the conductivity versus temperature plot we calculated the activation energy of NiO by using the following relations:

$$\sigma = \sigma_0 e^{-E_a/kT}$$

or

$$E_a = \{\ln(\sigma_0) - \ln(\sigma)\} \times kT$$

where σ represents the electrical conductivity, k the Boltzman constant and E_a is the activation energy. The details of σ_{RT} and activation energy have been furnished in Table 2. From Fig. 3 it can also be observed that the conductivity increases as temperature increases and nearly above 450 K the difference of conductivity between different partial pressure of O_2 was very little.

Non-stoichiometric nickel oxide is referred to as the p-type extrinsic semiconductors [30] in which vacancies

Table 2 Electrical conductivity at 300 K and activation energy at different oxygen percentages

Sample no	σ_{RT} (S cm^{-1})	E_a (meV)
NiO-(100%)	0.062	224
NiO-(80%)	0.0078	277
NiO-(70%)	0.0037	289
NiO-(50%)	6.14×10^{-5}	363

occurred at cation sites. For each cation vacancy there must be two holes formed. The overall reaction can be explained as bellow [31, 32]:

$$\frac{1}{2}O_2(g) \leftrightarrow O_o + V''_{Ni} + 2Ni'_{Ni}$$

where V''_{Ni} represents the Ni^{2+} vacancy and the $2Ni''_{Ni}$ act as Ni^{+3} ions. From the above relation it is clear that the defects, Ni^{2+} ion vacancies, are the cause for holes conductivity. Each vacancy of Ni^{2+} is replaced by two Ni^{3+} ions which increase the holes as carriers in NiO.

Figure 4 shows the schematic diagram of cation vacancy created due to non-stoichiometric NiO. It can be noticed that there is some excess oxygen comparing to the number of metal ions, but as a whole the total system is charge neutral. Therefore the holes are responsible for the electrical conductivity of the undoped NiO. Then finally nickel oxide, when it acts as a p-type material, can be written as [33]:

$$[Ni^{2+}_{1-3x}VNi^{3+}_{2x}]O$$

It was also shown that the electrical conductivity is proportional to the transfer of positive charge from cation to cation through the lattice [32, 34]. i.e.

$$\sigma \propto [Ni'_{Ni}]$$

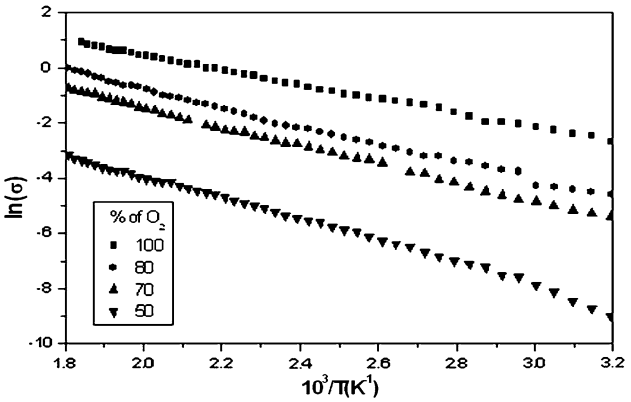

Fig. 3 $\ln(\sigma)$ versus $10^3/T$ plots of NiO thin film for different partial pressure of oxygen

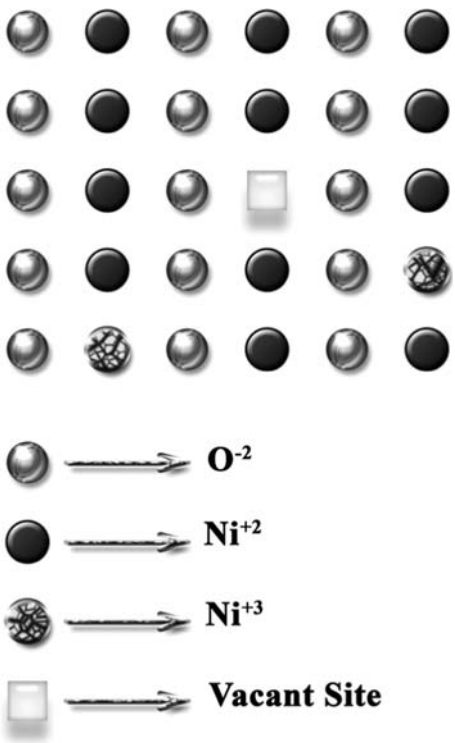

Fig. 4 Schematic diagram showing cation vacancies trapping positive holes (p) in non-stoichiometric NiO

Therefore the resistivity can be lowered by an increase of Ni^{3+} ions resulting from an addition of monovalent atoms such as lithium or by the creation of nickel vacancies and/or interstitial oxygen in NiO crystallites [35].

According to the Mattiessen's formula [36] the total resistivity [ρ_T] in the film is a result of various electrons scattering processes, which can be described by the following equation:

$$\rho_T = \rho_{Th} + \rho_I + \rho_D$$

where ρ_{TH}, ρ_I and ρ_D defined as thermal, impurity and defect resistivity respectively. At a constant temperature and for an undoped film, resistivity of NiO film is mainly determined by the defect resistivity component. From the previous explanation it can be said that this defect of NiO films is due to interstitial oxygen that occurs to create vacancies for Ni^{3+} ions. As a result, excess of oxygen in NiO creates vacancies in normally occupied Ni sites. To preserve overall electrical neutrality in the crystal, two Ni^{2+} ions must be converted to Ni^{3+} ions for each vacant Ni^{2+}. When an electron hops from a Ni^{2+} site to a Ni^{3+} site, it is as if a positive hole moves through the Ni^{2+} sites. Therefore NiO with excess of oxygen is p-type semiconductor [37]. To verify the above conjecture X-ray photoelectron

spectroscopic study was performed for the deposited NiO thin films.

X-ray photoelectron spectroscopic measurement

Figure 5 shows the XPS spectra corresponding to $Ni2p_{3/2}$ and $2p_{1/2}$ levels. The binding energies for $Ni2p_{3/2}$ and $2p_{1/2}$ were located at 855.55 eV and 873.53 eV respectively. For the O1s spectra peak at 530.6 eV was detected. It can be seen clearly, that the intensity of O1s peak is increasing with the higher amount of oxygen presence in the atmosphere at the time of deposition of NiO films. The binding energy of Ni^{2+} and Ni^{3+} of NiO and Ni_2O_3 are chosen to deconvolute the spectra of $Ni2p_{3/2}$. Here Ni^{3+} cations are for the defects occurred in non-stoichoimetric NiO. The binding energies of Ni^{2+} of NiO and Ni^{3+} of Ni_2O_3 for the $Ni2p_{3/2}$ peak are located around 854.6 eV and 857.2 eV [38] respectively. Figure 6a,b shows the deconvoluted peaks of Ni^{2+} and Ni^{3+} $2p_{3/2}$ peaks of non-stoichoimetric NiO films for complete oxygen and argon atmosphere respectively. As we have explained previously that the conductivity of NiO films is due to the defects structure of the non-stoichoimtric NiO, where Ni^{3+} cations are occupying the vacant positions of Ni^{2+} ions as oxygen partial pressure increases. The integrated peak area ratio of Ni^{+3}/Ni^{+2} (obtained from Fig. 6a, b) increases from 0.7 to 1.95 as oxygen partial pressure increases. These experimental results agreed with our schematic diagram and conductivity explanation.

UV–vis spectroscopic measurement

Figure 7 shows the transparency versus wavelength plot for different oxygen partial pressure in the sputtering gas mixture during deposition. It was seen that in the NIR region the transparency of NiO films are nearly about 75%.

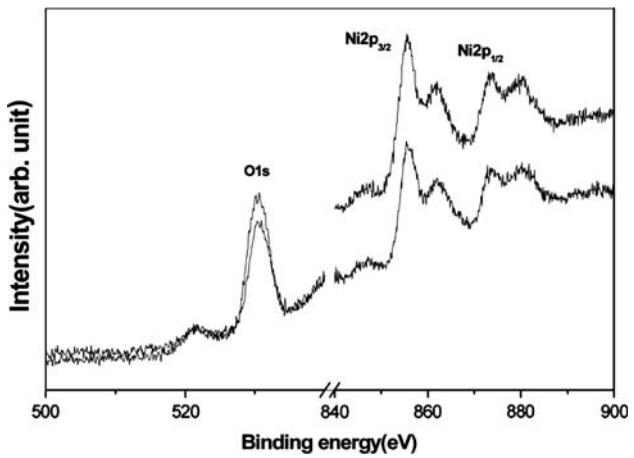

Fig. 5 XPS spectra of Ni2p and O1s for 100% O_2 and 100% Ar

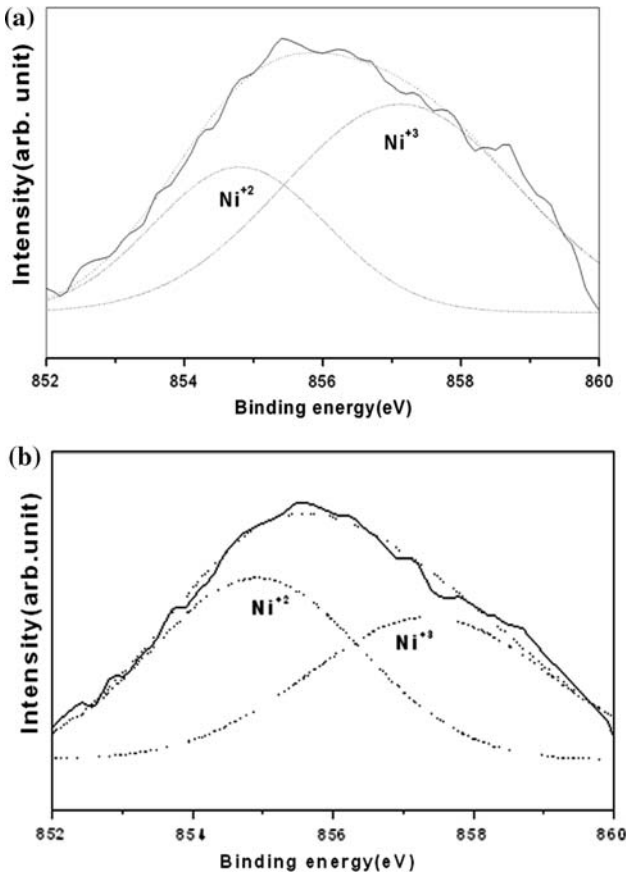

Fig. 6 Deconvolution of Ni^{+3} and Ni^{+2} of $Ni2p_{3/2}$ spectra of sputtered NiO films. (**a**) 100% O_2 and (**b**) 100% Ar atmosphere

From Fig. 7 it is also seen that with the increase of oxygen partial pressure the slope of the transmittance versus wavelength plot decreases, i.e. the spectrum becomes more

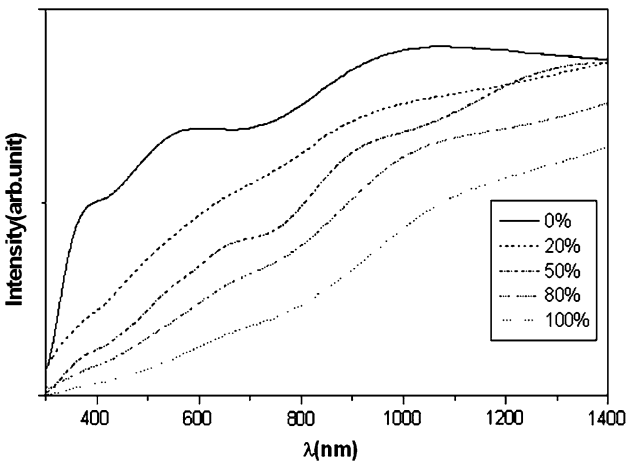

Fig. 7 Transmittance of NiO thin film for different partial pressure of oxygen

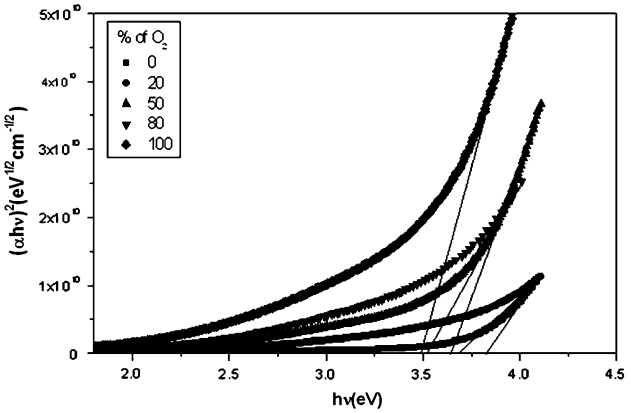

Fig. 8 Band gap variation of NiO thin film with different partial pressure of oxygen

flatter, which is due to the defects of non-stoichiometric NiO thin films [39].

The fundamental absorption that corresponds to the electron excitation from valance band to conduction band can be used to determine the nature and value of the optical band gap. The relation between the absorption coefficient (α) and the incident phonon energy ($h\nu$) can be written as [40]:

$$(\alpha h\nu)^{1/n} = A_n(h\nu - E_g)$$

where A_n is the constant, E_g correspond to the bandgap of the material and exponents n depends on the type of transition. For n = 1/2,2,3/2,3 values corresponding to allowed direct, allowed indirect, forbidden direct and forbidden indirect transition respectively. Figure 8 shows the $(\alpha h\nu)^2$ vs. ($h\nu$) plots for allowed direct transition. From the intercept on the energy axis by the extrapolation of the linear part of the curve $(\alpha h\nu)^2$ where $\alpha = 0$, the band gap E_g, of the NiO thin films were determined.

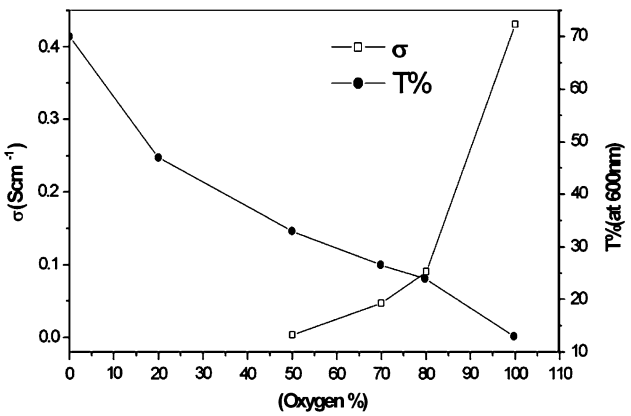

Fig. 9 Variation of conductivity and transparency of NiO thin film as a function of partial pressure of oxygen

Comparisons between conductivity and transmittance

Figure 9 shows the comparison between conductivity at 400 K and transparency of non-stoichoimetric NiO thin film at 600 nm deposited with different partial pressure of oxygen. The plot indicates that as the partial pressure of oxygen increases conductivity of NiO increases but transparency decreases. The reason behind it is that the defect states density of the NiO films increases due to excess oxygen.

Conclusions

NiO is a well-known metal deficient p-type semiconductor having wide bandgap and excellent chemical stability. Thin films of NiO (bunsenite) with (200) preferential orientation were synthesized on glass substrates by direct current sputtering technique in Ar + O_2 atmosphere. Electrical and optical properties of the films were investigated as a function of different partial pressure of oxygen in the sputtering gas mixture during deposition. It was shown that the films showed p-type electrical conduction and the conductivity depends on the partial pressure of oxygen. We also explained the cause behind the p-type conductivity of NiO films by defect chemistry. Corresponding optical properties showed that the transparency decreases with increasing oxygen partial pressure and also decreases the bandgap.

Acknowledgements The authors wish to thank Department of Science and Technology (DST), Govt. of India for financial support. The authors also wish to thank the University Grants Commission (UGC), Govt. of India, for providing some characterizational facilities under the 'University with potential for Excellence' scheme during the execution of the work. One of (BS) also wishes to thank UGC for awarding a junior research fellowship (JRF) during the execution of the work.

References

1. Swagten HJM, Strijkers GJ, Bloemen PJH, Willekens MMH, De Jonge WJM (1996) Phys Rev B 53:1039
2. Carey MJ, Berkowitz AE (1993) J Appl Phys 73:6892
3. Soeya S, Hoshiya H, Meguro K, Fukui H (1997) Appl Phys Lett 71:3424
4. Hwang DG, Lee SS, Park CM (1998) Appl Phys Lett 72:2162
5. Koide S (1965) J Phys Soc Jpn 20:123
6. Hotovy I, Huran J, Siciliano P, Capone S, Spiess L, Rehacek V (2001) Sens Actuators B Chem 78:126
7. Kumagai H, Matsumoto M, Toyoda K, Obara M (1996) J Mater Sci Lett 15:108
8. Kitao M, Izawa K, Urabe K, Komatsu T, Kuwano S, Yam S (1994) Jpn J Appl Phys 33:6656
9. Chan IM, Hsu TY, Hong FC (2002) Appl Phys Lett 81:1899
10. Nishizawa S, Tsurumi T, Hyodo H, Ishibashi Y, Ohashi N, Yamane M, Fukunaga O (1997) Thin Solid Films 302:133

11. Yu GH, Zeng LR, Zhu FW, Chai CL, Lai WY (2001) J Appl Phys 90:4039
12. Otterman CR, Temmink A, Bange K (1990) Thin Solid Films 193–194:409
13. Manago T, Ono T, Miyajima H, Yamaguchi I, Kawaguchi K, Sohma M (2000) Thin Solid Films 374:21
14. Jiao Z, Wu MG, Qin Z, Xu H (2003) Nanotechnology 14:458
15. Chen X, Wu NJ, Smith L, Ignatiev A (2004) Appl Phys Lett 84:14
16. Terakura K, Williams AR, Oguchi T, Kübler J (1984) Phys Rev B 40:4734
17. Antolini E (1992) J Mater Sci 27:3335
18. Cox PA (1998) The electronic structure and chemistry of solids. Oxford Science Publications, Oxford. Chapter 5.3
19. Tuller HL (1981) In: Sørensen OT (ed) Nonstoichiometric oxides. Academic Press, San Diego, Chapter 6
20. Banerjee AN, Ghosh CK, Das S, Chattopadhyay KK (2005) Physica B 370:264
21. J.C.P.D.S. Powder Diffraction File Card 04-0850
22. Lee M, Seo S, Seo D, Jeong E, Yoo IK. Section j: multiferroics and graded ferroelectrics
23. Green DW, Reedy GT, Kay JG (1979) J Mol Spectrosc 78:257
24. Bauschlicher CW Jr, Nelin CJ, Bagus PS (1985) J Chem Phys 82:3265
25. Walch SP, Goddard WA III (1978) J Am Chem Soc 100:1338
26. Bauschlicher CW Jr (1985) Chem Phys 93:399
27. Friedman-Hill EJ, Field RW (1992) J Mol Spectrosc 155:259
28. Bauschlicher CW Jr, Maitre P (1995) Theor Chim Acta 90:189
29. Vicki DM, Jarrold CC (1998) J Chem Phys 108(5):1804
30. Kofstad P (1972) Non-stoichiometry, diffusion, and electrical conductivity in binarymetal oxidex. Wiley, New York, p 252
31. Kofstad P (1972) Non-stoichiometry, diffusion, and electrical conductivity in binary metal oxidex. Wiley, New York, p 44
32. Kingery WD, Bowen HK, Ulhmann DL (1976) Introduction to ceramic, 2nd edn. Wiley, New York, p 899
33. Rees ALG (1954) Chemistry of the defect solid state. John Wiley and sons Inc., New York
34. Fogler HS (1992) Elements of chemical reaction engineering, 2nd edn. Prentice-Hall, New York, p 254
35. Dirksen JA, Duval K, Ring TA (2001) Sens Actuators B 80:106
36. Dummer GWA (1970) Materials for conductive and resistive function. Hayden Book Company Inc., New York
37. Walter JM (1967) Seven solid states. Benjamin, New York
38. Wanger CD, Riggs WM, Davis LE, Moulder JF (1979) Handbook of X-ray photoelectron spectroscopy. PHI, Eden Prairie, Minnesota
39. Lu YM, Hwang WS, Yang JS, Chuang HC (2002) Thin Solid Films 420–421:54
40. Pankove JI (1971) Optical process in semiconductors. Prentice Hall, Inc., New Jersey, p 34